# An Iterative Interference Cancellation Method for Co-Channel Multicarrier and Narrowband Systems

Mustafa E. Şahin [a] Ismail Guvenc [b] Hüseyin Arslan [a]

[a] *Electrical Engineering Department, University of South Florida, 4202 E. Fowler Ave., ENB-118, Tampa, FL, 33620,*
*E-mails: msahin@mail.usf.edu and arslan@eng.usf.edu.*

[b] *DOCOMO Communications Laboratories USA, Inc., 3240 Hillview Avenue, Palo Alto, CA, 94304*
*E-mail: iguvenc@docomolabs-usa.com.*

**Abstract**

Coexistence of narrowband (NB) and multicarrier technologies will be a major concern in next generation wireless communication systems due to the co-channel interference (CCI) problem. In this paper, an efficient CCI cancellation method is proposed that may be utilized for improved coexistence of NB and multicarrier technologies. The method treats both co-channel signals as desired signals and enhances them in an iterative manner. In every iteration, the signals are demodulated, regenerated, and subtracted from the received signal successively in order to obtain a better estimate of the other co-channel signal. Computational complexity of the proposed method is compared in detail with the joint demodulation technique. Through computer simulations, it is shown that the proposed method has lower complexity compared to joint demodulation, and it yields significant gains in the symbol error rate (SER) performance of both the NB and multicarrier systems.

*Key words:* CDMA, Co-channel interference, Femtocell, NBI, OFDMA, Successive interference cancellation.

## 1 Introduction

Transition from third generation (3G) to the fourth generation (4G) wireless systems is a major challenge that will be faced in the near future. Two different physical (PHY) layer technologies that have a high chance of being employed by next generation systems are Long Term Evolution (LTE) and WiMAX,

both of which are multicarrier (MC) systems and can have a bandwidth up to 20 MHz. Relative to these technologies, 3G systems such as EDGE, DECT, CDMA-2000, and even W-CDMA with its 5 MHz bandwidth need to be considered as narrowband (NB) systems. During the transition phase from 3G to 4G, various multicarrier and NB systems might have to share the same spectrum, which will result in a severe performance degradation in both systems due to the co-channel interference (CCI).

Suppression of narrowband interference (NBI) in OFDM systems has already been considered in several works in the prior-art [1]- [9]. In [1], linear minimum mean-square error (LMMSE) estimates of the interference are utilized. The proposed algorithm requires a priori information about the power spectral density of the NB signal. In [2], a normalized least mean squares (N-LMS) adaptive noise cancellation algorithm is introduced for suppressing NBI in pilot symbol assisted OFDM systems. NBI rejection via interferometry spreading codes is proposed in [3], whereas in [4, 5], a prediction error filter (PEF) is introduced in order to mitigate the effect of narrowband interference in the time domain. The NBI in an OFDM system has been addressed through successive interference cancellation methods in [6, 7]. In [6], assuming that the first subcarrier in consideration is interference-free, an error term is detected and used to mitigate the interference in subsequent subcarriers. This may result in error propagation in subsequent subcarriers in case of any error in the interference estimate. A generalization of the idea in [6] is discussed in [7] using soft decisions of the OFDM symbols. Two different NBI detection and cancellation algorithms using compressive sensing techniques have been proposed in [8], which show important gains in the OFDM bit error rate performance with respect to no cancellation. In [9], the NB signal is estimated over the unused OFDM subcarriers to cancel the NBI over the used OFDM subcarriers. The feasibility of this method is limited in practice due to the very few number of unused subcarriers in a well designed OFDM based system.

In this paper, we treat both co-channel signals as desired signals and propose a method that combats CCI through enhancing both signals in an iterative manner. In the literature, iterative co-channel interference cancellation techniques have been considered in [10]- [16], which typically assume narrowband systems and consider that the interferer and victim both use the same technology. In [10], it is emphasized that by exploiting the differences in signal features such as their delays, initial signal separation can be obtained, which considerably increases the efficiency of iterative interference cancellation. In the current paper, we exploit the inherent initial signal separation that exists due to the multicarrier vs. single carrier natures of interfering signals as well as the fact that the information is in frequency domain for MC signal and in time domain for NB signal. The proposed method assumes availability of signal reception and transmission capabilities for both systems. At each iteration, each signal is demodulated and then regenerated based on the symbol

decisions and the channel impulse response. This way, a better estimate of the signal is obtained. The regenerated signal is subtracted from the aggregate signal to obtain an estimation of the other co-channel signal. Through extensive simulations, it is proved that this method can provide a fundamental improvement in the performances of both systems in as few as three iterations. The relatively high computational burden (associated with multiple transitions between time and frequency domains) as well as the extra cost caused by the addition of a second system's transceiver functionalities are compensated by the fundamental performance gain obtained. Our other contributions include a detailed comparison of the computational complexity of the proposed method with the joint demodulation technique and evaluation of the Gaussian approximation (GA) method for characterizing the interference from the other system.

The paper is organized as follows: Section 2 provides application examples and the system models for the MC and NB systems in consideration. Also, it shortly discusses the GA based symbol error rate (SER). Section 3 reviews the joint demodulation technique for the NB and MC signals, while Section 4 is a detailed description of the proposed CCI cancellation method. A complexity comparison of the joint demodulation and iterative interference cancellation approaches is made in Section 5, simulation results are presented in Section 6, and the last section concludes the paper.

## 2 Application Examples and System Model

### *2.1 Application Examples*

Earlier examples of coexistence studies in the prior art include [17] and [18], which investigate the coexistence of code division multiple access (CDMA) and GSM systems. A contemporary example scenario, where coexistence of NB and multicarrier systems might be unavoidable, is the co-channel deployment of wideband CDMA (W-CDMA) based femtocells with LTE based macrocells, which has not been studied in the literature to our best knowledge. Femtocells [19, 20] are miniature cellular networks that have a communication range in the order of 10 meters. They can coexist with a macrocell network through either a split-spectrum approach, which leads to an inefficient spectrum utilization, or a shared-spectrum approach [21]- [23], where CCI is a potential concern. The initial deployments of femtocells will be mostly based on CDMA based technologies, such as the W-CDMA. In the future, while macro-cellular networks migrate to wider-band multicarrier-based technologies such as LTE, it might be expected that it takes a longer time for the consumers to replace their existing 3G femtocells with their next-generation versions. Hence, an

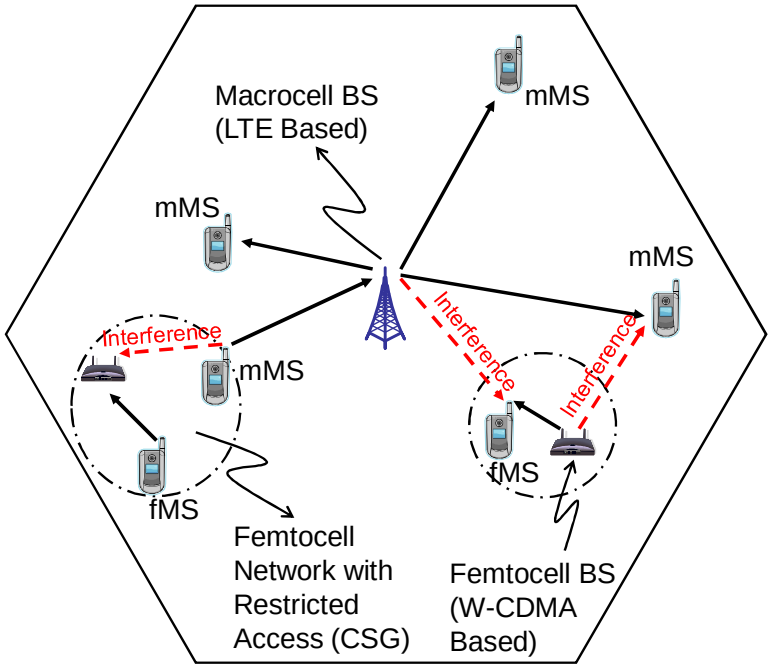


Fig. 1. An example coexistence scenario for an LTE based macrocell with a W-CDMA based femtocell during migration from 3G to 4G.

LTE based macrocell may need to coexist with a large number of 3G femtocells within its coverage area. In a shared-spectrum deployment, this would result in an interference from the macrocell at a femtocell, as illustrated in Fig. 1, which needs to be cancelled at the femtocell for an improved performance. Similarly, a W-CDMA femtocell may be interfering to an LTE based mobile station (MS) nearby, which again needs to be mitigated at the MS.

A particularly important scenario where interference cancellation may yield good gains for femtocell networks is for the restricted operation mode [1] of femtocells, where, the macrocell mobile stations (mMSs) are not allowed to make hand-off to the femtocell network even when the signal quality is superior at the femtocell [24, 25]. As illustrated in Fig. 1, this may result in significant uplink interference from the mMS to the femtocell BSs (fBSs), and significant downlink interference from the fBS to the mMSs. As discussed before, for the interference cancellation to become effective, the interference should be sufficiently strong; therefore, femtocells with restricted access are a good application scenario for interference cancellation techniques.

Another related example is the coexistence of multicarrier based ultra-wideband (UWB) systems (see e.g., [26]) with the relatively narrowband technologies (e.g., W-CDMA, bluetooth [27], etc.) [2]. It has been shown in [29] that multi-

[1] Also referred as the closed subscriber group (CSG) operation.

[2] Note that 60 GHz technologies as in [28] also have multicarrier transmission as an option and may face similar coexistence problems. Several other scenarios for

band orthogonal frequency division multiplexing (MB-OFDM) interference may seriously degrade the performance of NB systems at low signal-to-interference ratios (SIRs). While detect-and-avoid (DAA) approaches as in [30] are possible solutions for coexistence, it may not always be feasible to reliably detect the interference. Also, joint use of the spectrum may be more efficient in several scenarios if interference cancellation techniques can be successfully deployed. These scenarios include applications in the ISM bands where MC systems like WiFi coexist with NB systems, such as cordless phones and bluetooth devices.

### *2.2 System Model*

In this paper, two different co-channel interference scenarios are considered. The first scenario involves a MC and NB coexistence, and the second one deals with a MC and CDMA systems coexistence. The MC system employed has an orthogonal frequency division multiple accessing (OFDMA) based PHY layer. In both scenarios, it is assumed that the transceiver functionalities of both co-channel systems are available, but the primary receiver is the OFDMA receiver, i.e. perfect time and frequency synchronization to the OFDMA signal is ensured. This fact is illustrated in the diagram in Fig. 2, which shows the NB and OFDMA signals in time and frequency domains. It is demonstrated that synchronizing to the OFDMA symbols rather than NB symbols is necessary even if a targeted packet of NB symbols starts and ends somewhere in the middle of the OFDMA symbols.

Note that as discussed in [31], synchronization to the OFDM signal in the presence of NBI may be challenging, especially at low SIRs and large interference bandwidths. On the other hand, while [31] studies the impact of NBI on the synchronization error, techniques for improving the synchronization accuracy under the influence of NBI are also available in the literature (see e.g., [32]). Even though ideal synchronization is assumed in the present paper, in a more realistic setting, iterative synchronization approaches as in [32] may also be considered to capture synchronization errors.

The sampled downlink OFDMA signal in time domain can be written as [33]

$$x(n) = \sqrt{P_{\text{tx}}} \sum_{k=0}^{N-1} X(k) e^{j2\pi kn/N}, -N_{\text{cp}} \leq n \leq N-1, \tag{1}$$

where $P_{\text{tx}}$ is the transmit power, $N$ is the number of subcarriers, $k$ is the subcarrier index, $N_{\text{cp}}$ is the length of the cyclic prefix (CP), and $X(k)$ is the data on the $k$th subcarrier.

---

the coexistence of a narrowband and multicarrier system may also be considered.

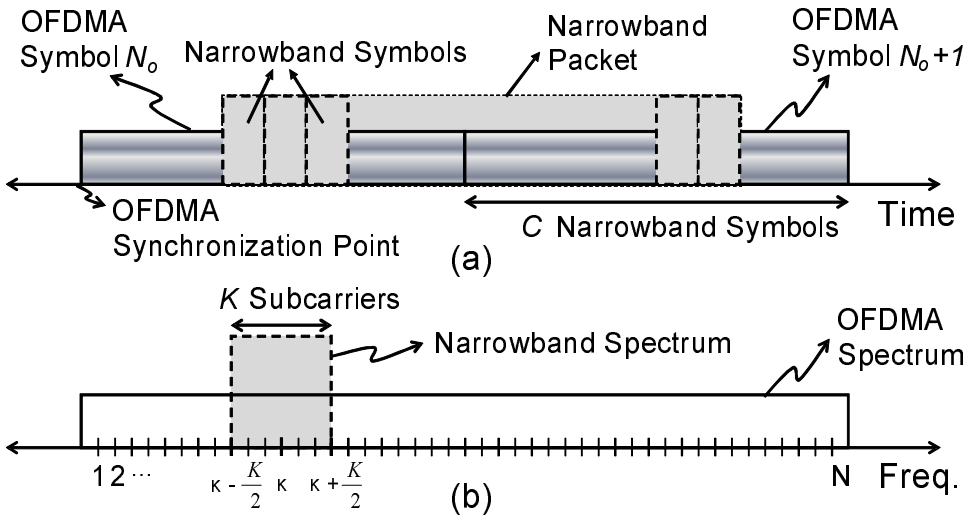


Fig. 2. Diagram of the OFDMA and NB symbols in time and frequency.

The received time domain OFDMA signal that traverses through a multipath channel $h(l)$ with $L_{\rm mc}$ taps is

$$y(n) = \sqrt{P_{\rm rx}} \sum_{l=0}^{L_{\rm mc}-1} h(l)x(n - D_l) \ , \tag{2}$$

where $P_{\rm rx}$ is the received signal power, and $D_l$ is the delay of the $l$th tap. Assuming that the maximum tap delay does not exceed the CP length, the frequency domain OFDMA signal can be shown as

$$Y(k) = \sqrt{P_{\rm rx}}X(k) \sum_{l=0}^{L_{\rm mc}-1} h(l)e^{-j2\pi kD_l/N} = \sqrt{P_{\rm rx}}X(k)H(k), \tag{3}$$

where $H(k)$ is the channel frequency response.

The baseband narrowband signal can be modeled as

$$s(n) = \sum_m a_m g(n - mT) \ , \tag{4}$$

where $m$ is the symbol index, $a_m$ denotes the $m$th data symbol, $g(n)$ is the pulse shaping filter with a roll-off factor $\alpha$, and $T$ is the symbol duration of the narrowband signal. In case of a CDMA signal, $s(n)$ becomes [34]

$$s(n) = \sum_m a_m g(n - mT)p(n - mT) \ , \tag{5}$$

where $p(n)$ is the spreading chip sequence with $R_{\rm c}$ chips. Since $s(n)$ passes through a multipath channel $h'(l)$ with $L_{\rm nb}$ symbol-spaced taps [3], the received

[3] Note that the symbol-spaced equivalent of any physical channel can be obtained by convolving the actual channel impulse response with the pulse shaping filter

signal becomes

$$z(n) = \sqrt{P_{\text{rx}}} \sum_{l=0}^{L_{\text{nb}}-1} h'(l)s(n - lT) \ . \tag{6}$$

The discrete Fourier transform (DFT) of $z(n)$ will be denoted as $Z(k)$. The main lobe of the spectrum occupied by $Z(k)$ overlaps with $K$ subcarriers of $Y(k)$ (see e.g., Fig. 2 and Fig. 5). Hence, if the center frequency of $Z(k)$ is located at subcarrier $\kappa$, the subcarriers $k \in \left[\kappa - \frac{K}{2}, \kappa + \frac{K}{2} - 1\right]$ will constitute the overlapping band (OB).

In time domain, NB symbols constitute structured information from a finite alphabet, while OFDMA signal behaves like random noise spread over multiple NB symbols. In frequency domain, on the other hand, OFDMA subcarriers carry structured information, and NB signal can be considered like random and colored noise covering multiple subcarriers. This is readily seen from the received signal, which can be denoted in time domain as

$$r(n) = \overbrace{z(n)}^{\text{NB}} + \underbrace{\overbrace{\sum_{k=0}^{N-1} Y(k)e^{j2\pi kn/N}}^{\text{OFDMA}}}_{y(n)} + w(n), \tag{7}$$

where $w(n)$ is the additive white Gaussian noise (AWGN) with a two sided power spectral density of $N_0/2$, and in frequency domain as

$$R(k) = \overbrace{Y(k)}^{\text{OFDMA}} + \underbrace{\overbrace{\frac{1}{N}\sum_{n=0}^{N-1} z(n)e^{-j2\pi kn/N}}^{\text{NB}}}_{Z(k)} + W(k), \tag{8}$$

where $W(k)$ is the frequency domain reciprocal $w(n)$.

### *2.3 Gaussian Approximation Based Symbol Error Rate*

The symbol error rate of a system under the effect of co-channel interference can be estimated assuming that the interfering signal amplitude has a Gaussian distribution, which is known as Gaussian approximation. The SER for a system employing QPSK modulation and using the GA is given by [35]

$$P_{QPSK} = 2Q\left(\sqrt{\frac{E_b}{\frac{N_0}{2} + \sigma_I^2}}\right)\left[1 - \frac{1}{2}Q\left(\sqrt{\frac{E_b}{\frac{N_0}{2} + \sigma_I^2}}\right)\right] , \tag{9}$$

employed and taking symbol-spaced samples.

where $Q$ denotes the Q-function, $E_b$ is the bit energy, and $\sigma_I^2$ is the interference variance, which is equal to $P_{\text{rx}}$ of the interfering signal.

The GA is rather simple but it is typically not very accurate especially at high SNR values where the resulting SER tends to be optimistic. For the scenario at hand, based on (7) and (8), the interference is a sum of $N$ random variables. Therefore, from the central limit theorem, this implies that GA for the specific scenario in consideration would be accurate (especially for large $N$). The accuracy of the GA is tested in a practical co-channel interference scenario by comparing it with actual simulation results in Section 6.

## 3 Joint Demodulation Method

A well-known and efficient method for handling co-channel signals is to demodulate them jointly utilizing maximum likelihood estimation [36, 37]. For the coexistence scenario in consideration, ML estimation might be performed either in time domain or in frequency domain. However, time domain requires a smaller number of computations and it is more desirable to perform the ML estimation in time domain. This is due to the relationship between $K$ and the number of NB symbols within the OFDMA symbol $C$, which can be written as $K = (1 + \alpha)C$, where $\alpha$ is usually greater than 0.

Denoting the estimates for the NB and OFDMA signals in time domain as $\hat{z}(n)$ and $\hat{y}(n)$, respectively, an ML estimate of both signals can be obtained as

$$\begin{aligned}\left[\hat{a}_m, \hat{X}(k)\right] &= \arg \min_{a_m, X(k)} \left\{ \left| r(mT) - z(mT) - y'(mT) \right|^2 \right\} \\ &= \arg \min_{a_m, X(k)} \left\{ \left| r(mT) - \sum_{l=0}^{L_{\text{nb}}-1} h'(l) a_{m-l} - \sum_{k=\kappa-\frac{K}{2}}^{\kappa+\frac{K}{2}-1} Y(k) e^{j2\pi kmT/N} \right|^2 \right\},\end{aligned} \tag{10}$$

where $y'(n)$ is the time domain reciprocal of $Y(k)$ for $k \in \left[\kappa - \frac{K}{2}, \kappa + \frac{K}{2} - 1\right]$.

The number of different values that $z(mT)$ and $y'(mT)$ can take should be limited in order for the joint demodulation algorithm to be computationally feasible. This condition is satisfied for both $z(mT)$ and $y'(mT)$ since the data sequences $a_m$ and $X(k)$ each belong to a finite alphabet. There are $M^K$ possibilities for the OFDMA signal in the overlapping band, and $M$ possibilities for each of the $C$ symbols in the NB signal, where $M$ is the number of constellation points depending on the modulation order (e.g., $M = 4$ for QPSK). Therefore, the number of possibilities that need to be considered for each NB

symbol is $M^{K+1}$.

Implementing (10) requires an exhaustive search through $M^{K+1}$ possible combinations of $z(mT)$ and $y'(mT)$, which are obtained by applying the channel responses to all possible values of $a_m$ and $X(k)$ to yield $z(mT)$ and $Y'(k)$, respectively, and also by computing the inverse DFT (IDFT) for all $Y'(k)$s to get $y'(mT)$s. This exhaustive search as well as the computations required for obtaining $z(mT)$ and $y'(mT)$s render the joint demodulation method prohibitively complex as it will be clearly demonstrated in Section 5.

## 4 Iterative CCI Cancellation Method

Considering the apparently high complexity of the ML estimation based joint demodulation method, we propose an efficient but low complexity alternative, which we call iterative CCI cancellation method. The iterative cancellation method solves the co-channel interference problem through enhancing both $Y(k)$ and $z(n)$ in a successive manner in multiple iterations. The iterations get started by obtaining and using an initial estimate of either $z(n)$ or $Y(k)$, which will be denoted as $\hat{z}(n)$ and $\hat{Y}(k)$, respectively.

An initial rough estimation for $z(n)$ can be obtained utilizing $Z(k)$ if the power of $Z(k)$ is high enough that it can be sensed over the OB through energy detection. The threshold of the energy detector is set according to the average signal-to-noise ratio (SNR) level over $k \notin \left[\kappa - \frac{K}{2}, \kappa + \frac{K}{2} - 1\right]$. In case the number of subcarriers whose energy exceeds the threshold is close to $K$, an initial estimate for the NB signal is obtained by taking the IDFT of the subcarriers $k \in \left[\kappa - \frac{K}{2}, \kappa + \frac{K}{2} - 1\right]$ to yield

$$\hat{z}(n) = \sum_{k=\kappa-\frac{K}{2}}^{\kappa+\frac{K}{2}-1} R(k) e^{j2\pi kn/N}. \tag{11}$$

If the NB signal is too weak to provide a useful estimate, or if $K$ is unknown, then, following an alternative approach, $R(k)$ is used as an initial estimate for $Y(k)$.

The main idea of the proposed method is to demodulate the estimated signal, $\hat{z}(n)$ or $\hat{Y}(k)$, and then to regenerate the signal waveform based on the symbol decisions made to obtain $\tilde{z}(n)$ or $\tilde{Y}(k)$. Note that $\tilde{z}(n)$ and $\tilde{Y}(k)$ are expected to be cleaner versions of $\hat{z}(n)$ and $\hat{Y}(k)$, respectively, since they are free of AWGN and supposedly less affected by CCI.

Since the initial estimate employed $\left(\hat{z}(n) \text{ or } \hat{Y}(k)\right)$ is corrupted by CCI and AWGN, the symbol decisions made may include errors. However, the effect

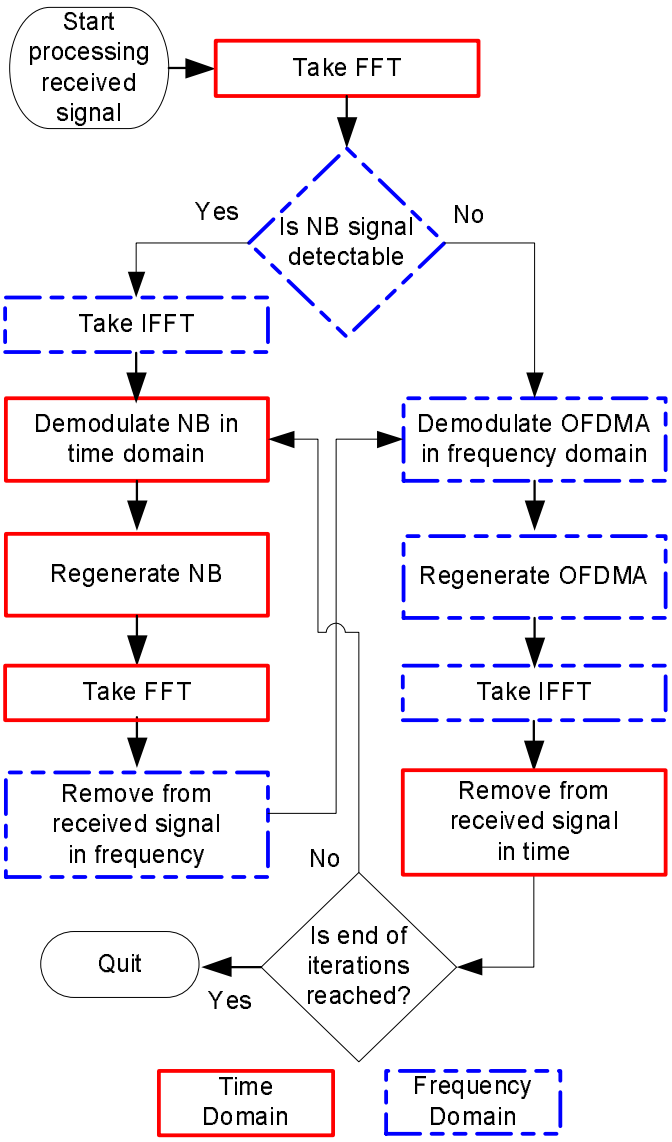


Fig. 3. Flowchart of the proposed iterative CCI cancellation algorithm.

of symbol errors made in $\hat{z}(n)$ is not localized in frequency domain; on the contrary, it is spread over $K$ subcarriers. Similarly, a corrupted subcarrier in $\hat{Y}(k)$ has an impact that is spread over $N$ samples in time domain. Hence, subtracting $\tilde{z}(n)$ with symbol errors from $r(n)$ does not necessarily corrupt subcarriers of $\hat{Y}(k)$. The same is true when $\tilde{Y}(k)$ with some incorrectly demodulated subcarriers is removed from $R(k)$; it does not necessarily lead to a $\hat{z}(n)$ with symbol errors.

The flowchart provided in Fig. 3 illustrates the steps that need to be followed after obtaining the initial signal. The first step is demodulation. The internal stages for demodulation are shown for the NB system in a separate flowchart in Fig. 4. It starts with downconverting the signal to the baseband from the intermediate frequency (IF) of $f_c' - f_c$, where $f_c$ and $f_c'$ are the carrier frequen-

cies of the OFDMA signal and the NB signal, respectively. If the NB signal is a CDMA signal, this stage is followed by multiplication with the pseudo-noise (PN) sequence, which is shown with a dashed block in Fig. 4. The rest of demodulation is performed by applying channel equalization, downsampling, and making symbol decisions to obtain the IQ data. For the NB system, it is assumed that the carrier frequency $f_c'$ is known, and a channel estimate $\hat{h}'(l)$ is available [4]. For the OFDMA system, downconversion and downsampling stages do not exist [5], and channel estimation is performed over pilot subcarriers to obtain $\hat{H}(k)$.

After obtaining the IQ data, regeneration (demonstrated for NB signal in Fig. 4) takes place. The steps that constitute regeneration are upsampling the IQ data, applying pulse shaping, (if the signal is a CDMA signal) multiplying the signal with the PN sequence, upconverting it, and convolving it with the baseband channel. Again, upsampling and upconversion are not performed for the OFDMA signal. The pulse shaping filter used by the NB system is assumed to be known. If the regenerated signal is $\tilde{z}(n)$, its DFT is taken, and the resulting signal $\tilde{Z}(k)$ is removed from $R(k)$ to obtain an estimate for the OFDMA signal, i.e.

$$\hat{Y}(k) = R(k) - \tilde{Z}(k) = R(k) - \frac{1}{N}\sum_{n=0}^{N-1} \tilde{z}(n)e^{-j2\pi kn/N}. \tag{12}$$

If the regenerated signal is $\tilde{Y}(k)$, its IDFT is taken, and the resulting signal $\tilde{y}(n)$ is subtracted from $r(n)$ to obtain an estimate for the NB signal as follows

$$\hat{z}(n) = r(n) - \tilde{y}(n) = r(n) - \sum_{k=0}^{N-1} \tilde{Y}(k)e^{j2\pi kn/N}. \tag{13}$$

[4] The proposed algorithm's performance for an NB system with channel estimation errors is investigated through simulations in Section 6.

[5] The received signal $r(n)$ is already downconverted to the baseband based on the carrier frequency $f_c$ of the OFDMA signal.

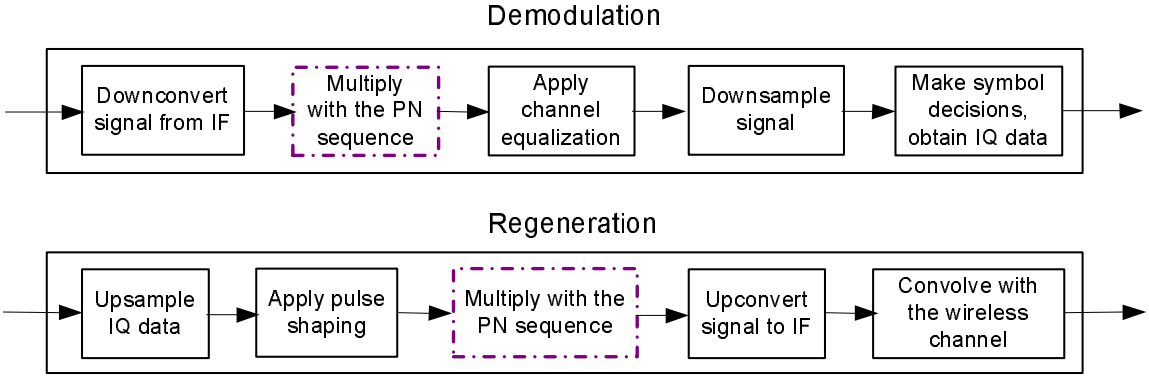


Fig. 4. Flowchart of the demodulation and regeneration modules for the NB system.

An important question that might be raised about the proposed method is why the entire OFDMA band is handled rather than dealing with the OB only, because processing the entire band has the following disadvantages:

- Since $\tilde{y}(n)$ is the IDFT of the entire OFDMA band rather than the OB only, any errors made in the demodulation of subcarriers $k \notin \left[\kappa - \frac{K}{2}, \kappa + \frac{K}{2} - 1\right]$ appear as additive noise in (13). It would be expected that this increases the number of NB demodulation errors, especially if $K$ is small,
- The complexity of the algorithm becomes proportional to $N$ rather than $K$ (as it will be analyzed in Section 5).

The reasons why we do not deal with the OB only is that $K$ may not always be known accurately, and also, subcarriers $k \notin \left[\kappa - \frac{K}{2}, \kappa + \frac{K}{2} - 1\right]$ might have been affected by the sidelobes of the NB signal. Moreover, through computer simulations, it is found that the extra noise caused by the demodulation errors outside the OB does not lead to a noticeable increase in the NB demodulation errors even for $\frac{K}{N}$ ratios as small as 2.5%.

As it will be shown in Section 6, both iterative cancellation and ML detection observe a *hunch* effect in their SER performance curves. That is because interference cancellation works effectively if either the desired signal or the interference is strong and can be separated easily from the received signal. When the strengths of the two signals are close to each other a hunch is observed in the performance results, which can be described as follows: 1) The bit-error-rate (BER) performance improves with the increasing signal to interference ratio (SIR) for low SIR values, 2) It starts degrading with the increasing SIR for moderate interference levels and gets worse when the interference power is comparable with the desired signal power, and 3) BER starts improving again as the SIR increases further. The hunch effect may also be theoretically analyzed using the asymptotic efficiency. As discussed in [38], the asymptotic efficiency of a single-user receiver goes to zero as the interference power increases. On the other hand, for an optimum detector, there exists a point where the interference is strong enough to be demodulated accurately, and asymptotic efficiency starts improving (reader is referred to [38] for further theoretical treatment). Due to the hunch effect, it can be argued that interference cancellation is most useful when the interference is very strong.

## 5 Computational Complexity

Co-channel interference needs to be canceled in real-time by a mobile station or a base station that is affected by CCI. Therefore, the computational complexity of the cancellation algorithm employed is critical. This section aims to provide a comparison of complexities of the maximum likelihood and the pro-

posed iterative interference cancellation algorithms in terms of the CPU cycle counts required by multiplication (MUL), addition (ADD), and comparison (CMP) operations.

### *5.1 ML Method*

According to the information provided in Section 3, there are $M^K$ possibilities for $K$ interfered subcarriers in the OFDMA signal, and $M$ possibilities for each of the $C$ NB symbols. Applying the channel frequency response to the possible OFDMA symbols requires $M^K K$ complex MULs. Applying the channel impulse response to $C$ NB symbols, on the other hand, requires $MC$ convolutions, where each convolution is equivalent to $L$ complex MULs and $L-1$ complex ADDs.

After appyling the channel responses, all possible OFDMA signals need to be transfered from frequency domain into the time domain via $M^K$ inverse fast Fourier transform (IFFT) operations of size $N$. Each IFFT operation requires $\frac{N}{2}\log_2 N$ complex MULs and $N\log_2 N$ complex ADDs. Adding the OFDMA and NB signals and subtracting their sum from the received signal requires $2M^{K+1}C$ complex ADDs. To obtain the absolute squared differences for all possibilities, $2M^{K+1}C$ MULs and $M^{K+1}C$ ADDs are performed. The minimum of the $M^{K+1}$ absolute squared values obtained is found performing $M^{K+1}$ CMPs for all $C$ NB symbols.

Taking into account that a complex ADD is equivalent to 2 real ADDs, and a complex MUL is equal to 4 real MULs and 2 real ADDs, the computations required can be listed in terms of real MULs, real ADDs, and CMPs as in Table 1.

### *5.2 Iterative Cancellation*

In the proposed iterative cancellation method, for a desired number of iterations $\mathcal{I}$, $2(1+\mathcal{I})$ FFT and IFFT operations need to be performed in total, each of which requires $\frac{N}{2}\log_2 N$ complex MULs and $N\log_2 N$ complex ADDs. To find whether the NB signal is detectable over the OB, the absolute squared values for $K$ samples in frequency domain need to be calculated and compared with a threshold value. These two operations are performed via $2K$ MULs plus $K$ ADDs, and $K$ CMPs, respectively.

In each of the $\mathcal{I}$ iterations desired, to demodulate the OFDMA subcarriers, $N$ complex MULs are needed for equalization and $N\log_2 M$ CMPs for making symbol decisions . For the demodulation of NB symbols, if a maximum likeli-

hood sequence estimation (MLSE) equalizer is employed, $4CLM^L$ MULs and $CM^L(4L-2)$ ADDs are needed (according to [39]), whereas a linear equalizer (LE) such as a zero-forcing equalizer (ZFE) or an MMSE equalizer would require $CL$ complex MULs and $C(L-1)$ complex ADDs. Also, $C\log_2 M$ CMPs are necessary for making symbol decisions.

Again in each iteration, to regenerate the OFDMA subcarriers, $N$ complex MULs are needed to apply the wireless channel effect. In NB symbols' regeneration, on the other hand, a convolution is required for applying the channel, which is equal to $CL$ complex MULs and $C(L-1)$ complex ADDs, and another convolution for pulse shaping, which is equal to $2CN$ MULs and $2(C-1)N$ ADDs. Finally, in each iteration each of the subtractions from the received signal in time and in frequency require $N$ complex ADDs. The computations required for each step of the iterative cancellation method are provided in the second part of Table 1.

Table 1
The Computations Required for Maximum Likelihood and Iterative Cancellation Algorithms

| | Operation | MUL | ADD | CMP |
|---|---|---|---|---|
| **Maximum Likelihood** | **Applying Channel Responses** | $4M^K K + 4MCL$ | $2M^K K + 2MC(2L-1)$ | |
| | **Taking IFFT** | $2M^K N\log_2 N$ | $3M^K N\log_2 N$ | |
| | $\boldsymbol{r(n) - \left(\hat{z}(n) + \hat{y}(n)\right)}$ | | $4M^{K+1}C$ | |
| | $\boldsymbol{\lvert.\rvert^2}$ | $2M^{K+1}C$ | $M^{K+1}C$ | |
| | $\boldsymbol{\min(\lvert.\rvert^2)}$ | | | $M^{K+1}C$ |
| **Iterative Cancellation** | **Taking FFT/IFFT** | $4(1+\mathcal{I})N\log_2 N$ | $6(1+\mathcal{I})N\log_2 N$ | |
| | **Energy Detection** | $2K$ | $K$ | $K$ |
| | **OFDMA Equalization** | $4\mathcal{I}N$ | $2\mathcal{I}N$ | |
| | **NB Equalization (MLSE)** | $4\mathcal{I}CLM^L$ | $\mathcal{I}CM^L(4L-2)$ | |
| | **NB Equalization (LE)** | $4\mathcal{I}CL$ | $2\mathcal{I}C(2L-1)$ | |
| | **Symbol Decision** | | | $\mathcal{I}(N+C)\log_2 M$ |
| | **Applying Channel Responses** | $4\mathcal{I}N + 4\mathcal{I}CL$ | $2\mathcal{I}N + 2\mathcal{I}C(2L-1)$ | |
| | **Pulse Shaping** | $2\mathcal{I}CN$ | $2\mathcal{I}(C-1)N$ | |
| | $\boldsymbol{r(n) - \tilde{y}(n)}$ & $\boldsymbol{R(k) - \tilde{Z}(k)}$ | | $4\mathcal{I}N$ | |

Table 2
CPU Cycle Counts Obtained Using a XilinX DSP48 Slice

| **N** | **K** | **C** | **L** | **M** | $\mathcal{I}$ | **ML** | **Iter. I** | **Iter. II** |
|---|---|---|---|---|---|---|---|---|
| 512 | 40 | 32 | 4 | 4 | 3 | $5.3\times10^{28}$ | $2.3\times10^{6}$ | $7.9\times10^{5}$ |
| 512 | 20 | 16 | 4 | 4 | 3 | $4.7\times10^{16}$ | $1.3\times10^{6}$ | $5.8\times10^{5}$ |
| 512 | 10 | 8 | 4 | 4 | 3 | $4.4\times10^{10}$ | $8.6\times10^{5}$ | $4.8\times10^{5}$ |
| 512 | 40 | 32 | 4 | 16 | 3 | $7.0\times10^{52}$ | $3.9\times10^{8}$ | $7.9\times10^{5}$ |
| 512 | 40 | 32 | 4 | 4 | 5 | $5.3\times10^{28}$ | $3.8\times10^{6}$ | $1.3\times10^{6}$ |
| 512 | 40 | 32 | 1 | 4 | 3 | $5.3\times10^{28}$ | $7.8\times10^{5}$ | $7.8\times10^{5}$ |
| 1024 | 40 | 32 | 4 | 4 | 3 | $1.1\times10^{29}$ | $3.2\times10^{6}$ | $1.6\times10^{6}$ |

### *5.3 Comparison of Complexities*

A numerical comparison of complexities of the two algorithms in terms of CPU cycle counts can be obtained considering that the cycle numbers for ADD, MUL, and CMP operations, in a Xilinx DSP48 slice for instance, are 1, 3, and 1, respectively [40]. The CPU cycle counts determined for both algorithms employing various sets of system parameters are demonstrated in Table 2, where Iter. I stands for the iterative cancellation method employing an MLSE equalizer for the NB system, and Iter. II is the iterative method employing an LE.

In Table 2, it is observed that there is a drastic difference between the cycle numbers required for ML and Iter. I algorithms. This is caused by the fact that every step of the ML estimation has an exponential complexity, whereas Iter. I has a linear complexity except for the MLSE equalizer that it employs. Cycle counts for Iter. II algorithm show that the complexity of the iterative cancellation can be decreased further by employing a linear equalizer, especially when $M$ or $L$ is large.

It is seen that parameter $K$ (and $C$, which depends on $K$) acts exponentially on the complexity of ML estimation and linearly on the iterative cancellation. $M$ affects ML estimation and Iter. I exponentially, whereas it has a negligible effect on Iter. II. $N$ has a linear effect on all algorithms, and $\mathcal{I}$ has a linear effect on the iterative ones. $L$ has a relatively weak impact on ML estimation and Iter. II, whereas it affects Iter. I exponentially.

As a last note, the computation time required to run the iterative algorithm might be of significant importance. If the computation time is longer than the channel coherence time, there might be variations in the channel responses, and the performance might be considerably affected. Assuming a high speed

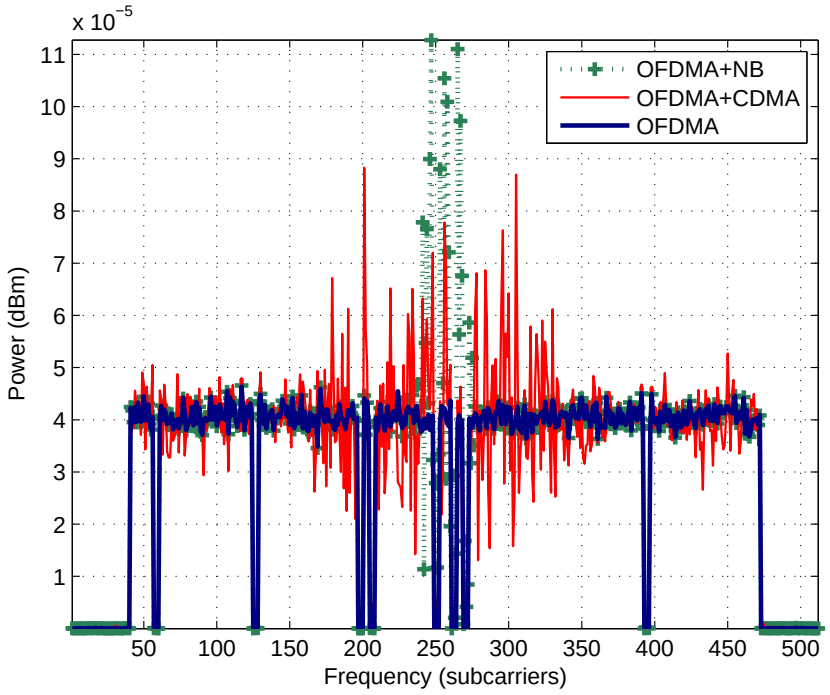


Fig. 5. The spectra of the received co-channel signals and the OFDMA signal alone (OFDMA SNR: 30 dB, NB SNR: 20 dB). CDMA spectrum is wider than the NB spectrum due to multiplication with the PN sequence.

platform such as Xilinx Virtex-4 FPGA that operates at 500 MHz and has 32 of DSP48 slices, the computation times required for Iter. I and Iter. II employing the parameters in the first row of Table 2 are 143.75 $\mu$s and 49.38 $\mu$s, respectively. Given that the channel coherence times at carrier frequencies 2.5 GHz and 5 GHz at a speed of 2 km/h are 200 ms and 93 ms, respectively, it can be conveniently claimed that the proposed algorithm will not suffer from such a problem.

## 6 Simulations

### *6.1 Simulation Parameters*

Computer simulations are done to determine the performance of the proposed iterative canceler in different scenarios as well as to compare it with the joint demodulation method's performance. For the simulations, a custom simulator prepared in MATLAB was utilized. The parameters of the OFDMA, NB, and CDMA systems employed in the simulations are presented in Table 3. The OFDMA symbol occupies 400 subcarriers out of 512 available ones due to the guard bands and empty subcarriers. The overlapping band, which is lo-

cated in the middle of the OFDMA spectrum, is approximately 40 subcarriers wide for the NB signal, and 128 subcarriers wide for the uplink CDMA signal (illustrated in Fig. 5).

The SER performances of OFDMA, NB, and CDMA systems are investigated both in AWGN (Figs. 6-9) and multipath (MP) (Figs. 10-13) channels. In MP simulations, availability of a perfect channel estimation is assumed for NB and CDMA, and an efficient MLSE equalizer is utilized. For OFDMA, on the other hand, pilot based practical channel estimation and equalization are performed. In all simulations, while the desired signal power is varied over a certain range, noise power is fixed, and interference SNR is kept constant. Signal-to-interference-plus-noise ratio (SINR) is defined as the ratio of the desired signal power to the sum of interference and noise power over the overlapping band.

In Figs. 6-13, the uppermost curve shows the performance obtained without applying CCI cancellation (referred as "without cancellation"), whereas the lowest curve shows the performance when CCI does not exist (referred as "No CCI"). The three curves in between demonstrate the SER performances after each iteration [6]. The SINR values on the x-axis apply only to the without cancellation curve. As a last note, the no CCI curve is actually an SER vs. SNR curve shifted leftwards by the amount of interference SNR, which is 30 dB in Fig. 6 and Fig. 10; 25 dB in Fig. 7 and Fig. 11; 20 dB in Fig. 8 and Fig. 12; and 15 dB in Fig. 9 and Fig. 13.

[6] In Fig. 12, the first two iterations are omitted, and the performance curves obtained for two different channel estimation error levels are displayed instead.

Table 3
OFDMA, Narrowband, and CDMA System Parameters

| **Parameter** | **OFDMA** | **Narrowband** | **CDMA** |
|---|---|---|---|
| **Bandwidth** | 5 MHz | 370 kHz | 625 kHz |
| **Samples per symbol** | 512 | 16 | 32 |
| **Modulation** | QPSK | QPSK | QPSK |
| **MP channel model** | Veh. A [41] | Out.-to-in. A [41] | Out.-to-in. A [41] |
| **Pulse shape** | Rectang. | Raised cos. ($\alpha$=0.3) | Raised cos. ($\alpha$=0.3) |

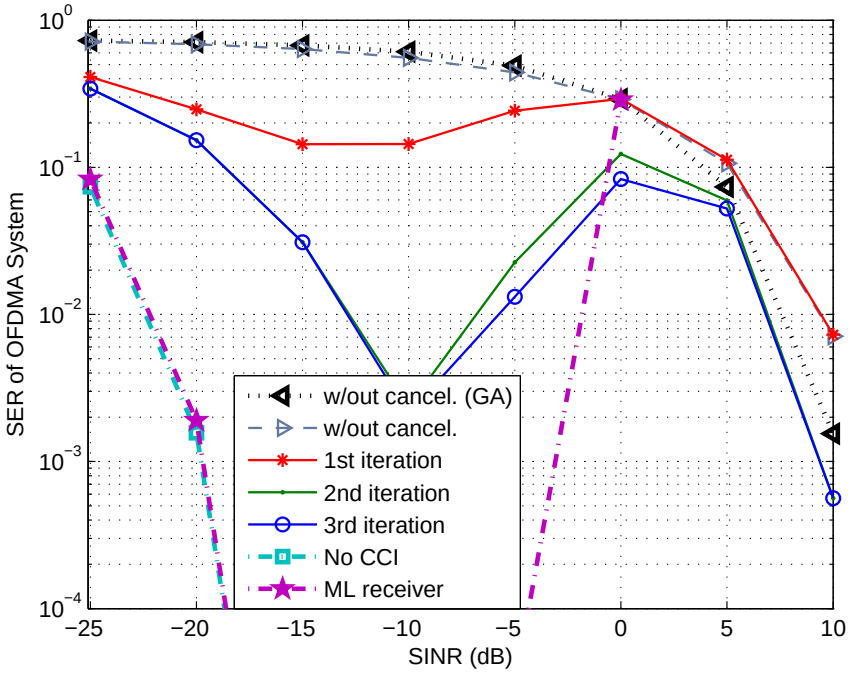


Fig. 6. SER performance of the OFDMA system under the influence of NB interference (AWGN channel).

### *6.2 AWGN Channel Results*

Fig. 6 shows the SER performance of the OFDMA system interfered by an NB system. At very low SINR levels, since the interfering signal can be detected accurately, the gain with respect to without cancellation can be as large as 25 dB after the 3rd iteration. As SINR approaches 0 dB, however, it becomes challenging to separate the two signals from each other, and the gain drops to around 6 dB. Beyond 10 dB SINR, the SER curve of the proposed method approaches to the without cancellation curve. This is reasonable because when the interference is too weak relative to the desired signal, interference cancellation is not expected to yield a high gain. It is worth to note that while there is a considerable gain difference between the first two iterations, the extra gain yielded by the third iteration is not that significant.

Fig. 6 also shows the theoretical performance curve that is obtained by using the GA for the co-channel interference. It is observed that the GA yields quite accurate values up until 0 dB SINR, after where it yields optimistic SERs. Another performance curve that is displayed in Fig. 6 belongs to the maximum likelihood receiver, whose SER is as low as the "No CCI" case at low SINR values. The ML receiver is superior to the iterative canceler everywhere except around 0 dB SINR, where ML has demodulation problems in AWGN channel [13].

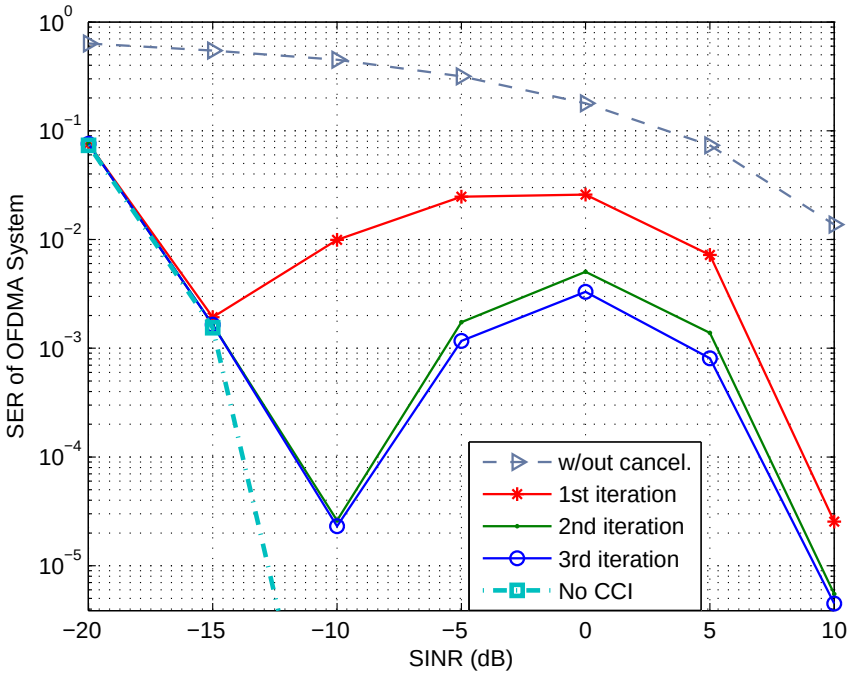


Fig. 7. SER performance of the OFDMA system under the influence of CDMA interference (AWGN channel).

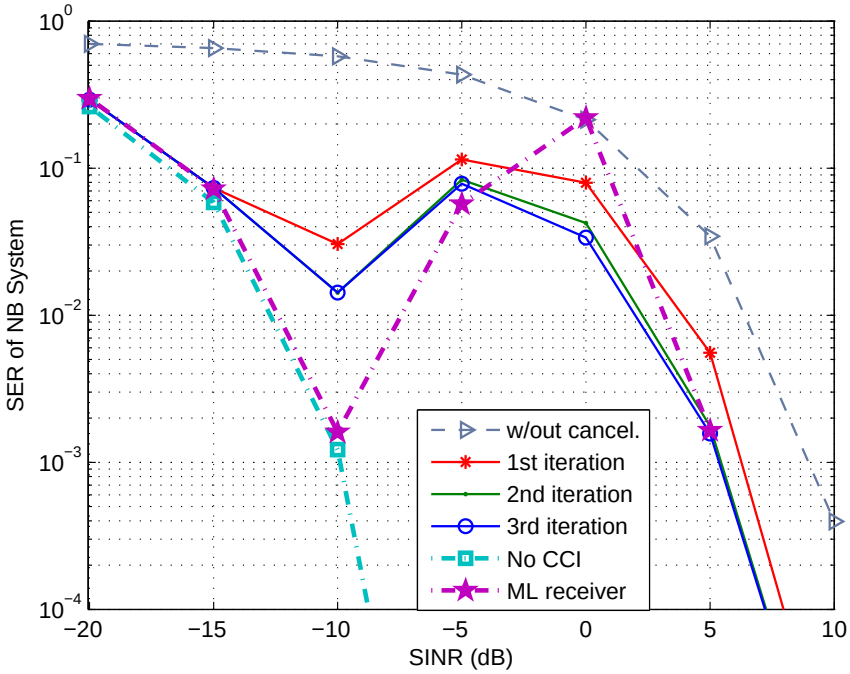


Fig. 8. SER performance of the NB system under the influence of OFDMA interference (AWGN channel).

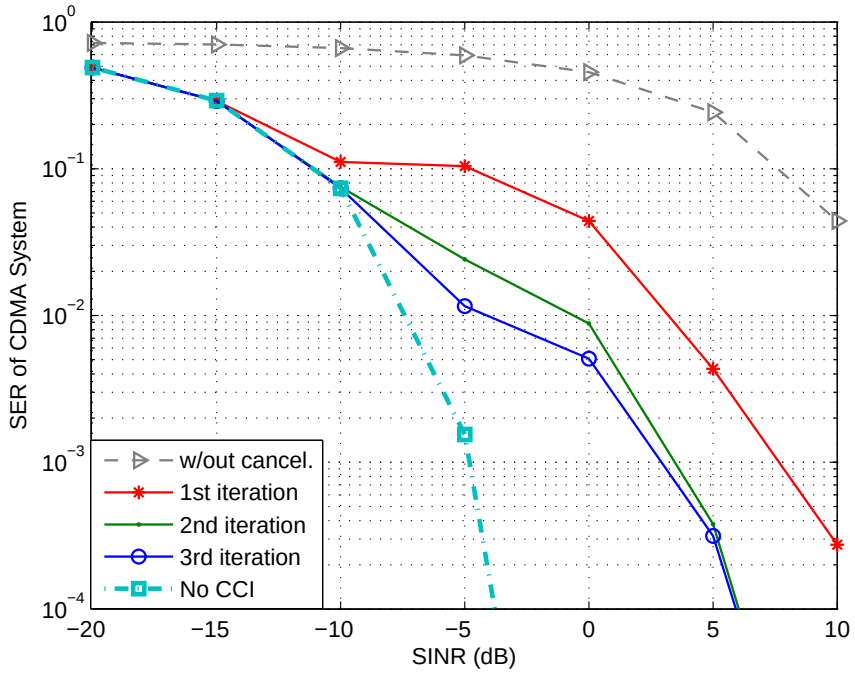


Fig. 9. SER performance of the CDMA system under the influence of OFDMA interference (AWGN channel).

In case of CDMA interference, the gains obtained for the OFDMA system, which are displayed in Fig. 7, are considerably larger than the previous case. The reason for this performance difference is the involvement of the PN sequence, which introduces additional signal separability. The fact that the CDMA signal power is spread over a wider frequency band (compared to the NB signal) makes the OFDMA signal more accurately detectable. Once the cancellation process starts with a reliable estimate for the OFDMA signal, the following iterations become more successful, as well.

The NB system performance improvement enabled by the proposed method is shown in Fig. 8. For SINR values smaller than 0 dB, the gain with respect to no CCI cancellation can be as high as 18 dB. For SINR greater than 0 dB, there is still a gain around 3 dB. Fig. 8 also shows the ML receiver performance. ML receiver is superior to the iterative canceler in general. However, at around 0 dB SINR, it yields apparently higher SER than the iterative canceler.

The improvement of the CDMA performance is again more significant as it can be seen in Fig. 9. The SER values are much closer to the no CCI curve at low SINR values, and there is a 10 dB gain even at rather high SINR.

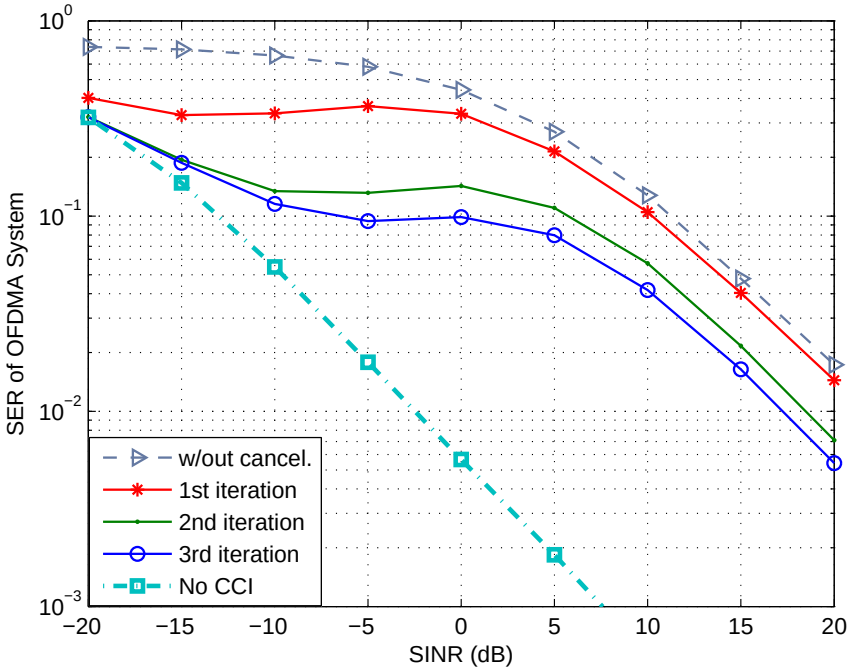


Fig. 10. SER performance of the OFDMA system under the influence of NB interference (MP channel).

### *6.3 Multipath Channel Results*

In MP simulation results in Figs. 10-13, the margin between without cancellation and no CCI curves is not as wide as in the AWGN case. Nevertheless, the proposed algorithm is still able to provide considerable gains. For the OFDMA system interfered by the NB signal (see Fig. 10), the gain is above 15 dB up until 0 dB SINR, after which it decreases towards 5 dB again. When the interferer is CDMA (see Fig. 11), on the other hand, the gains are considerably higher, and the performance curve approaches the no CCI case.

Improvement of the NB performance is shown in Fig. 12. The gain obtained for SINR smaller than 0 dB is more than 12 dB. Approaching 0 dB SINR, this gain becomes smaller, but even at 10 dB SINR there is still a gain of approximately 5 dB. Impact of NB channel estimation error on the performance of iterative cancellation is also demonstrated in Fig. 12. The variance of the Gaussian noise added to each channel tap estimate is set as a certain ratio of the power of that tap. The two ratios examined are 5% and 10%. It is observed that the cancellation gain decreases with increasing channel estimation error. Still, it can be stated that channel estimation errors, which are likely to occur under CCI effect, do not have a very strong influence at error levels as large as 5%.

The CDMA performance improvement (see Fig. 13) is more critical. The per-

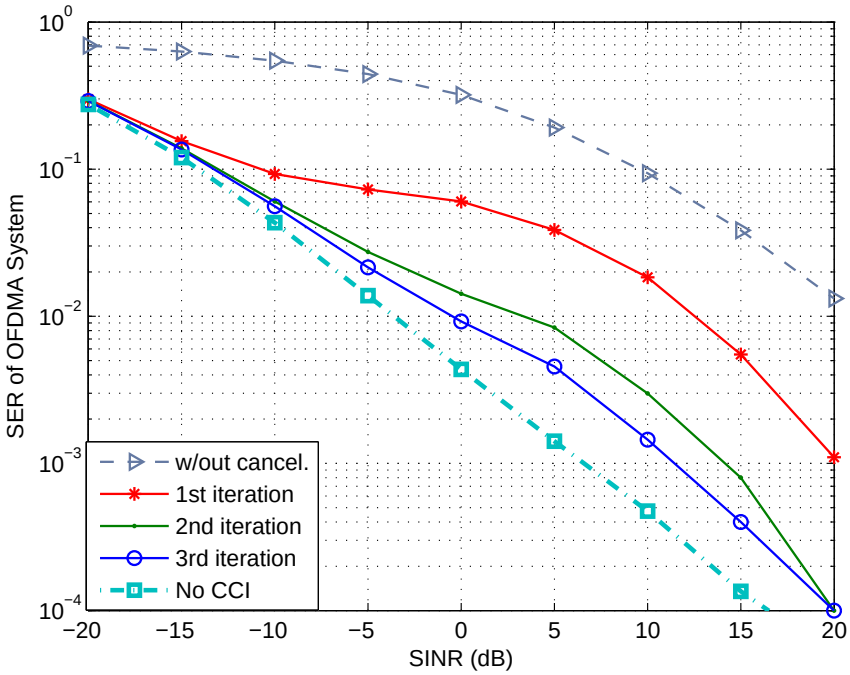


Fig. 11. SER performance of the OFDMA system under the influence of CDMA interference (MP channel).

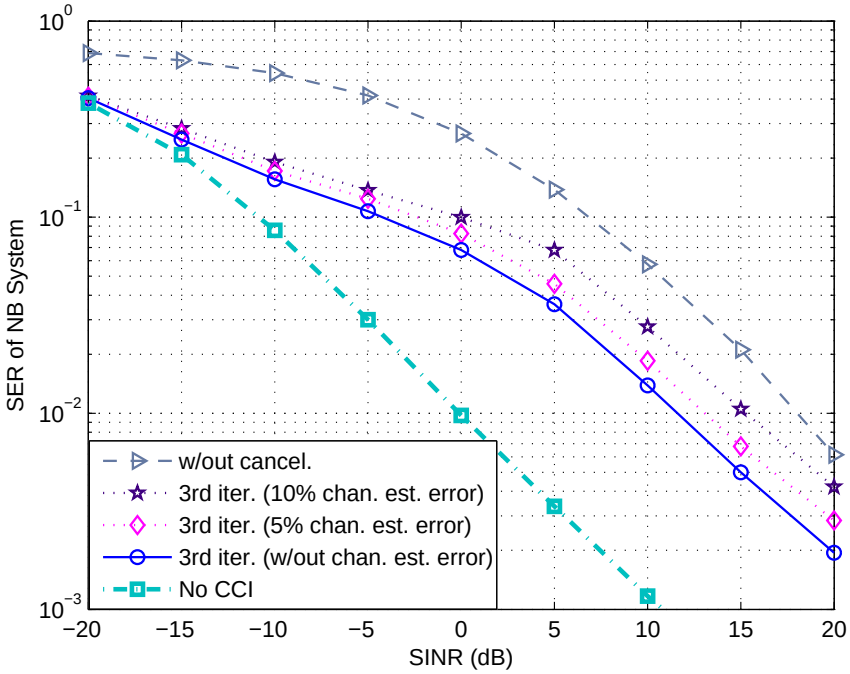


Fig. 12. SER performance of the NB system under the influence of OFDMA interference (MP channel).

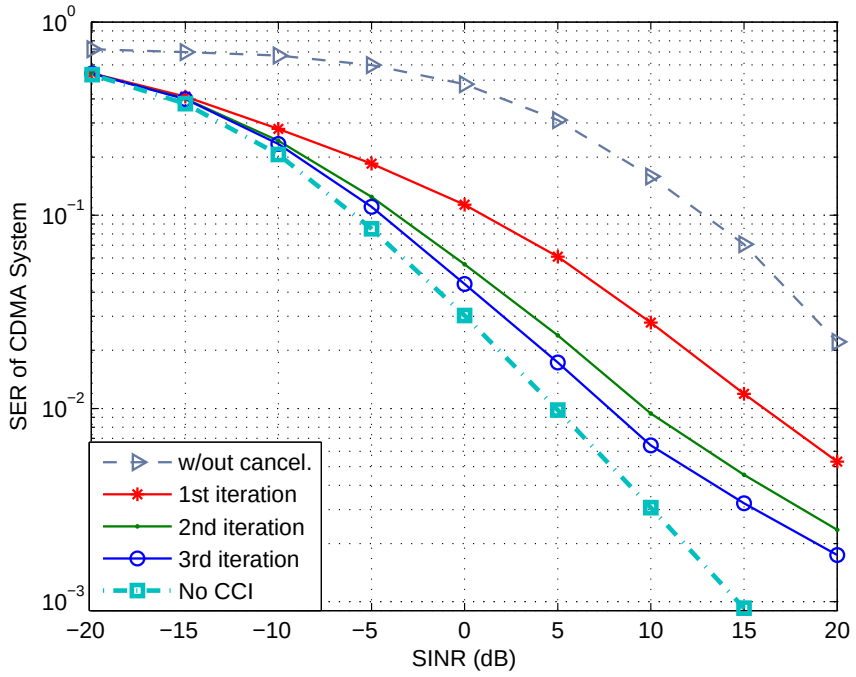


Fig. 13. SER performance of the CDMA system under the influence of OFDMA interference (MP channel).

formance is almost as good as no CCI case up until 0 dB SINR, after where it starts to decrease. The difference between the NB and CDMA curves' behavior is again due to the use of a PN sequence.

### *6.4 Effect of Overlapping Bandwidth*

The width of the OB has a considerable effect on the cancellation performance of the proposed iterative method. This effect is investigated in terms of SER values of the OFDMA system in Fig. 14, where the overlapping bandwidths are expressed as their ratio to the OFDMA signal bandwidth. The performance curves that are obtained for various overlap percentages clearly indicate that increasing overlap leads to a more successful cancellation. This is because, for a given SINR value, the energy of the NB signal changes linearly depending on its bandwidth, i.e. the NB signal in a widest overlap scenario is the strongest one. Increased NB signal energy leads to a more successful demodulation of the NB symbols, which in turn boosts the overall performance of the algorithm.

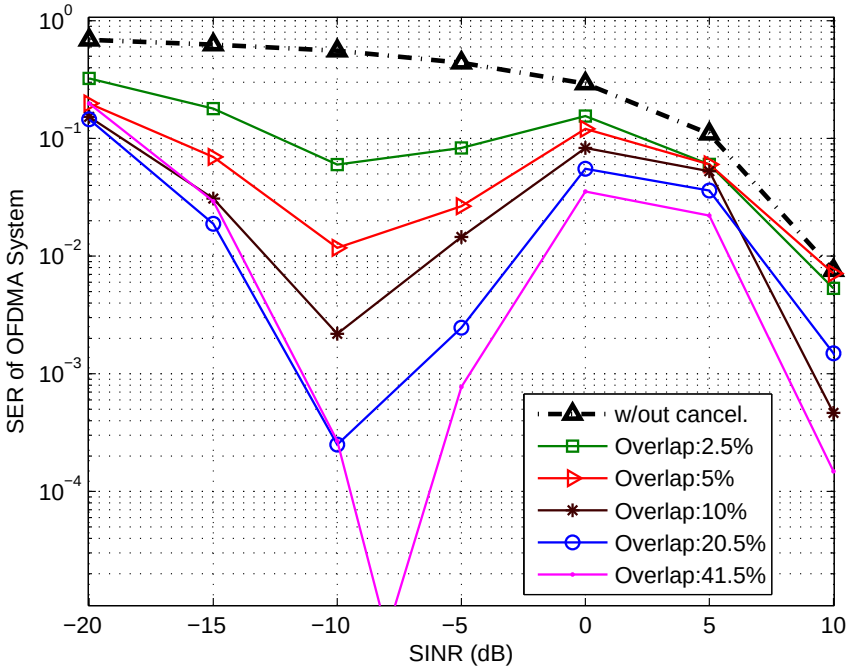


Fig. 14. OFDMA system's SER performance under the influence of NB interference for various overlapping bandwidths (AWGN channel).

### *6.5 Capacity of OFDMA Under NBI*

Besides obtaining the SERs for various scenarios, system capacity analysis was also performed to compare the system capacity obtained by the iterative cancellation algorithm to the capacity obtained by alternative methods. For obtaining the system capacities, a binary symmetric channel (BSC) was considered, which can be realized by introducing sufficient interleaving to the data bits to be transmitted. For a BSC, the channel capacity $X$ is given by [35]

$$X = P_b \log_2(2P_b) + (1 - P_b)\log_2 2(1 - P_b), \tag{14}$$

where $P_b$ is the BER. The system capacity is obtained by multiplying $X$ by the number of symbols per second and number of bits per symbol (as well as number of subcarriers for the OFDMA system).

In Fig.15, the capacity of the OFDMA system in the overlapping band is plotted, where an AWGN channel is considered. It is observed that compared to the capacity available without performing any cancellation, the capacity yield by the iterative cancellation is rather close to the capacity of the ML receiver. At around 0 dB SINR, the iterative cancellation yields the highest capacity because of the demodulation problem that the ML receiver suffers from as mentioned in subsection 6.2.

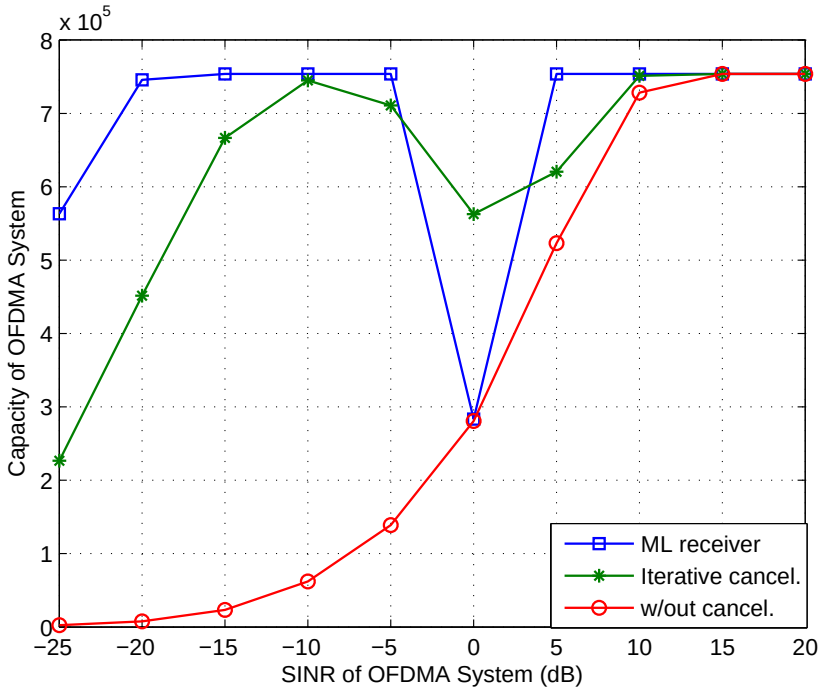


Fig. 15. Capacity of the OFDMA system in the overlapping band.

In Fig.16, the total capacity of the coexisting OFDMA and NB systems in the OB is demonstrated. Along with the ML receiver and iterative cancellation, the detect-and-avoid method is also investigated, which is a frequently considered technique for handling interference in coexistence scenarios. In the DAA method, the OFDMA system avoids using the entire OB when it detects that the interference power is equal or greater than its own received power [30]. NB system, on the other hand, does not perform avoidance regardless of its SINR level. The curves in Fig.16 show that the iterative cancellation algorithm's capacity is considerably higher than the DAA method's capacity, while it is quite close to the ML receiver's capacity exceeding it around 0 dB SINR.

## 7 Concluding Remarks

In this paper, an iterative CCI canceler is proposed that mitigates the NB interference in multicarrier spectrum as well as the effect of MC signal on NB symbols. Application scenarios are provided where the proposed canceler might be very attractive such as the coexistence of CDMA and OFDMA based systems during the migration from 3G to 4G wireless technologies. It is shown that processing the whole MC band rather than only the overlapping band is more advantageous in spite of the increased complexity. Moreover, it is numerically demonstrated that the proposed method is significantly less complex compared to joint demodulation. In the simulations, fundamental gains are ob-

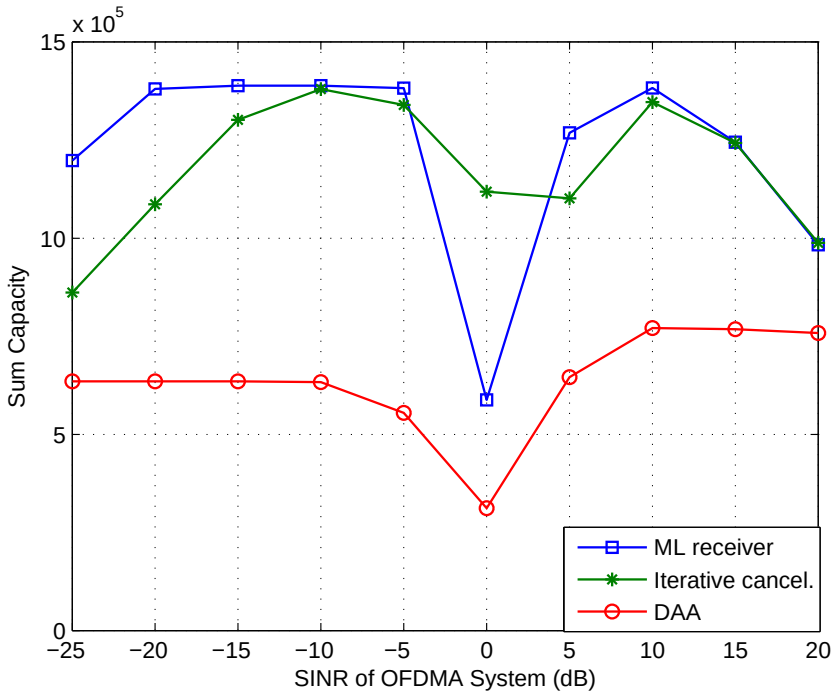


Fig. 16. Sum capacity of the coexisting OFDMA and NB systems in the overlapping band.

tained for both co-channel signals in terms of SER performance validating the claimed efficiency of the proposed method. Also, the effect of NB channel estimation errors on the available gains is quantified. Finally, it is found that larger gains are possible when the overlap between the NB and MC signals is larger.

## References

[1] R. Nilsson, F. Sjoberg, and J. LeBlanc, "A rank-reduced LMMSE canceller for narrowband interference suppression in OFDM-based systems," *IEEE Trans. Commun.*, vol. 51, no. 12, pp. 2126–2140, Dec. 2003.

[2] A. Coulson, "Narrowband interference in pilot symbol assisted OFDM systems," *IEEE Trans. Commun.*, vol. 3, no. 6, pp. 2277–2287, Nov. 2004.

[3] Z. Wu and C. Nassar, "Narrowband interference rejection in OFDM via carrier interferometry spreading codes," *IEEE Trans. Commun.*, vol. 4, no. 4, pp. 1491–1505, July 2005.

[4] A. Batra and J. Zeidler, "Narrowband interference mitigation in BICM OFDM systems," in *Proc. IEEE Int. Conf. on Acoustics, Speech and Signal Proc. (ICASSP)*. Taipei, Taiwan: IEEE Computer Soc., Apr. 2009, pp. 2605–2608.

[5] ——, "Narrowband interference mitigation in OFDM systems," in *Proc. IEEE Military Commun. Conf. (MILCOM)*, San Diego, CA, Nov. 2008, pp. 1–7.

[6] D. Darsena, "Successive narrowband interference cancellation for OFDM systems," *IEEE Commun. Letters*, vol. 11, no. 1, pp. 73–75, 2007.

[7] D. Darsena and F. Verde, "Successive NBI Cancellation Using Soft Decisions for OFDM Systems," *IEEE Signal Proc. Letters*, vol. 15, 2008.

[8] A. Gomaa, K. Z. Islam, and N. Al-Dhahir, "Two novel compressed-sensing algorithms for NBI detection in OFDM systems," in *Proc. IEEE Int. Conf. on Acoustics, Speech and Signal Proc. (ICASSP)*, Dallas, TX, Mar. 2010.

[9] D. Zhang, P. Fan, and Z. Cao, "A novel narrowband interference canceller for OFDM systems," in *Proc. IEEE Wireless Commun. and Network. Conf. (WCNC)*, vol. 3, Mar. 2004, pp. 1426–1430.

[10] H. Arslan and K. Molnar, "Cochannel interference suppression with successive cancellation in narrow-band systems," *IEEE Commun. Lett.*, vol. 5, no. 2, pp. 37–39, 2001.

[11] X. G. Doukopoulos and R. Legouable, "Intercell interference cancellation for MC-CDMA systems," in *Proc. IEEE Vehic. Technol. Conf. (VTC)*, Dublin, Ireland, Apr. 2007, pp. 1612–1616.

[12] M. Mohaisen and K. H. Chang, "Maximum-likelihood co-channel interference cancellation with power control for cellular OFDM networks," in *Proc. Int. Symp. on Commun. Inform. Technol. (ISCIT)*, Sydney, Australia, Oct. 2007, pp. 198–202.

[13] H. Yoshino and A. Czylwik, "Adaptive co-channel interference (CCI) cancellation for OFDM communication systems," in *Proc. Int. Zurich Seminar on Broadband Commun.*, Zurich, Switzerland, Feb. 2000, pp. 245–250.

[14] P. A. Hoeher, S. B. Hoeher, W. Xu, and C. Krakowski, "Single-antenna co-channel interference cancellation for TDMA cellular radio systems," *IEEE Wireless Commun. Mag.*, vol. 12, no. 2, pp. 30–37, Apr. 2005.

[15] M. Shibahara, T. Fujii, I. Sasase, and T. Saba, "Performance evaluation of adaptive co-channel interference canceling receiver using frequency spread coding and frequency interleaving for OFDM systems," *European Trans. Telecommun.*, vol. 14, pp. 15–24, Jan. 2003.

[16] H. Schoeneich and P. Hoeher, "Iterative semi-blind single-antenna cochannel interference cancellation and tight lower bound for joint maximum-likelihood sequence estimation," *Elsevier Signal Proc.*, vol. 84, no. 11, pp. 1991–2004, 2004.

[17] P. Kaczorek and D. Rutkowski, "A comparison of narrowband and broadband overlay of cellular CDMA on GSM," in *Proc. IEEE Vehic. Technol. Conf. (VTC)*, vol. 3, May 2000, pp. 1859–1863.

[18] R. Sahota and P. Whiting, "On the feasibility of spectrum sharing between GSM and IS-95," in *Proc. IEEE Personal Wireless Commun.*, Mumbai, India, Dec. 1997, pp. 439–443.

[19] L. T. W. Ho and H. Claussen, "Effects of user-deployed, co-channel femtocells on the call drop probability in a residential scenario," in *Proc. IEEE Int. Symp. Personal, Indoor and Mobile Radio Commun. (PIMRC)*, Athens, Greece, Sep. 2007, pp. 1–5.

[20] H. Claussen, "Performance of macro- and co-channel femtocells in a hierarchical cell structure," in *Proc. IEEE Int. Symp. Personal, Indoor and Mobile Radio Commun. (PIMRC)*, Athens, Greece, Sep. 2007, pp. 1–5.

[21] V. Chandrasekhar and J. G. Andrews, "Uplink capacity and interference avoidance for two-tier cellular networks," in *Proc. IEEE Global Telecommun. Conf. (GLOBECOM)*, Washington, DC, Nov. 2007, pp. 3322–3326.

[22] V. Chandrasekhar, J. Andrews, and A. Gatherer, "Femtocell networks: a survey," *IEEE Commun. Mag.*, vol. 46, no. 9, pp. 59–67, September 2008.

[23] I. Guvenc, M.-R. Jeong, F. Watanabe, and H. Inamura, "A hybrid frequency assignment for femtocells and coverage area analysis for co-channel operation," *IEEE Commun. Lett.*, vol. 12, no. 12, pp. 880–882, Dec. 2008.

[24] "3rd Generation Partnership Project; Technical Specification Group Radio Access Networks; 3G Home NodeB Study Item Technical Report (Release 8)," 3GPP, 3GPP TR 25.820, March 2008.

[25] FemtoForum, "Interference management in UMTS femtocells," White Paper, Dec. 2008. [Online]. Available: http://www.femtoforum.org/femto/Files/File/Interference Management in UMTS Femtocells.pdf

[26] ECMA International, "High rate ultra wideband PHY and MAC," ECMA-368 Standard, Dec. 2008. [Online]. Available: http://www.ecma-international.org/publications/files/ECMA-ST/ECMA-368.pdf

[27] J. Park, D. Kim, C. Kang, and D. Hong, "Effect of Bluetooth interference on OFDM-based WLAN," in *Proc. IEEE Vehic. Technol. Conf. (VTC)*, vol. 2, Orlando, FL, Oct. 2003.

[28] ECMA International, "High rate 60 GHz PHY, MAC, and HDMI PAL," ECMA-387 Standard, Dec. 2008. [Online]. Available: http://www.ecma-international.org/publications/files/ECMA-ST/ECMA-387.pdf

[29] A. Nasri, R. Schober, and L. Lampe, "Analysis of narrowband communication systems impaired by MB-OFDM UWB interference," *IEEE Trans. Wireless Commun.*, vol. 6, no. 11, pp. 4090–4100, Nov. 2007.

[30] S. M. Mishra, R. W. Brodersen, S. T. Brink, and R. Mahadevappa, "Detect and avoid: an ultra-wideband/WiMAX coexistence mechanism," *IEEE Commun. Mag.*, vol. 45, no. 6, pp. 68–75, June 2007.

[31] M. Marey and H. Steendam, "Analysis of the narrowband interference effect on OFDM timing synchronization," *IEEE Trans. Sig. Processing*, vol. 55, no. 9, pp. 4558–4566, Sep. 2007.

[32] A. Aghajeri and H. Shafiee, "Synchronization in OFDM powerline communication systems in presence of narrowband interferences," in *Proc. IEEE Int. Symp. Signal Processing and Its Appl.*, vol. 2, Jul. 2003, pp. 359–362.

[33] L. Cimini, "Analysis and simulation of a digital mobile channel using orthogonal frequency division multiplexing," *IEEE Trans. Commun.*, vol. 33, no. 7, pp. 665–675, 1985.

[34] A. Viterbi *et al.*, *CDMA: principles of spread spectrum communication*. Addison-Wesley Reading, MA, 1995.

[35] J. G. Proakis, *Digital Communications*, 4th ed. New York: McGraw-Hill, 2001.

[36] P. Ranta, A. Hottinen, and Z.-C. Honkasalo, "Co-channel interference cancelling receiver for TDMA mobile systems," in *Proc. IEEE Int. Conf. Commun. (ICC)*, vol. 1, Seattle, WA, Jun. 1995, pp. 17–21.

[37] H. Schoeneich and P. Hoeher, "Single antenna interference cancellation: iterative semiblind algorithm and performance bound for joint maximum-likelihood interference cancellation," in *Proc. IEEE Global Telecommun. Conf. (GLOBECOM)*, vol. 3, Dec. 2003, pp. 1716–1720.

[38] S. Verdu, *Multiuser Detection*. 1st ed. Cambridge, UK: Cambridge University Press, 1998, ch. 4, p. 184.

[39] Y. Kopsinis and S. Theodoridis, "An efficient low-complexity technique for MLSE equalizers for linear and nonlinear channels," *IEEE Trans. Signal Process.*, vol. 51, no. 12, pp. 3236–3248, Dec. 2003.

[40] H. Mahmoud, H. Arslan, and M. Ozdemir, "Initial Ranging for WiMAX (802.16e) OFDMA," in *Proc. IEEE Military Commun. Conf. (MILCOM)*, Washington, DC, Oct. 2006, pp. 1–7.

[41] ITU-R Recommendation M. 1225, "Guidelines for Evaluation of Radio Transmission Technologies for IMT-2000," 1997.